

RESEARCH ARTICLE

In vitro genotoxicity of dibutyl phthalate on A549 lung cells at air–liquid interface in exposure concentrations relevant at workplaces

Stephanie Binder^{1,2} | Xin Cao^{1,2} | Stefanie Bauer¹ | Narges Rastak¹ | Evelyn Kuhn¹ | George C. Dragan³ | Christian Monseé⁴ | George Ferron¹ | Dietmar Breuer⁵ | Sebastian Oeder¹ | Erwin Karg¹ | Martin Sklorz¹ | Sebastiano Di Bucchianico¹ | Ralf Zimmermann^{1,2}

¹Joint Mass Spectrometry Center at Comprehensive Molecular Analytics, Helmholtz Zentrum München, Neuherberg, Germany

²Joint Mass Spectrometry Center at Analytical Chemistry, Institute of Chemistry, University of Rostock, Rostock, Germany

³Federal Institute for Occupational Safety and Health (BAuA) – Measurement of Hazardous Substances, Dortmund, Germany

⁴Institute for Prevention and Occupational Medicine of the German Social Accident Insurance (IFA), Institute of the Ruhr-Universität Bochum (IPA), Bochum, Germany

⁵Institute of Occupational Safety of the German Social Accident Insurance (IFA), Sankt Augustin, Germany

Correspondence

Sebastiano Di Bucchianico, Joint Mass Spectrometry Center at Comprehensive Molecular Analytics, Helmholtz Zentrum München, Neuherberg, Germany.
Email: dibucchianico@helmholtz-muenchen.de

Funding information

German Social Accident Insurance (DGUV), Grant/Award Number: FP425

Accepted by: B. B. Gollapudi

Abstract

The ubiquitous use of phthalates in various materials and the knowledge about their potential adverse effects is of great concern for human health. Several studies have uncovered their role in carcinogenic events and suggest various phthalate-associated adverse health effects that include pulmonary diseases. However, only limited information on pulmonary toxicity is available considering inhalation of phthalates as the route of exposure. While in vitro studies are often based on submerged exposures, this study aimed to expose A549 alveolar epithelial cells at the air–liquid interface (ALI) to unravel the genotoxic and oxidative stress-inducing potential of dibutyl phthalate (DBP) with concentrations relevant at occupational settings. Within this scope, a computer modeling approach calculating alveolar deposition of DBP particles in the human lung was used to define in vitro ALI exposure conditions comparable to potential occupational DBP exposures. The deposited mass of DBP ranged from 0.03 to 20 ng/cm², which was comparable to results of a human lung particle deposition model using an 8 h workplace threshold limit value of 580 µg/m³ proposed by the Scientific Committee on Occupational Exposure Limits for the European Union. Comet and Micronucleus assay revealed that DBP induced genotoxicity at DNA and chromosome level in sub-cytotoxic conditions. Since genomic instability was accompanied by increased generation of the lipid peroxidation marker malondialdehyde, oxidative stress might play an important role in phthalate-induced genotoxicity. The results highlight the importance of adapting in vitro studies to exposure scenarios relevant at occupational settings and reconsidering occupational exposure limits for DBP.

KEYWORDS

air–liquid interface, alveolar deposition, dibutyl phthalate, genotoxicity, oxidative stress

This is an open access article under the terms of the Creative Commons Attribution-NonCommercial-NoDerivs License, which permits use and distribution in any medium, provided the original work is properly cited, the use is non-commercial and no modifications or adaptations are made.

© 2021 The Authors. *Environmental and Molecular Mutagenesis* published by Wiley Periodicals LLC on behalf of Environmental Mutagen Society.

1 | INTRODUCTION

Phthalates are environmental pollutants that are ubiquitous in air, dust, and food. Due to their technical properties, they are used in a broad range of industrial branches mainly as plasticizers in several synthetic polymers. Nevertheless, their potential adverse health effects are of great concern for human and environmental health (Warner & Flaws, 2018).

Phthalates have gained attention mainly due to their endocrine disruptive functions and their deleterious effects on embryonic development and reproductive systems (Zoeller et al., 2012). Several epidemiological and *in vivo* studies have associated phthalate exposure with an increased risk of developing asthma and allergy (Wang et al., 2019), structural impairment of the lung (Hou et al., 2020), and even cancer (Wang et al., 2012). Despite the fact that inhalation is an important route of phthalate exposure in workplace and indoor environment (Chi et al., 2017; Frery et al., 2020), few experimental studies consider inhalation as an entry route. Nevertheless, the effects of airborne phthalates on the development and promotion of lung diseases remain elusive and concern arises due to extensive airway exposure (Kashyap & Agarwal, 2018). As a consequence, only limited information on the pathophysiological effects of phthalates on lung function and structure is available and a solid link to respiratory diseases has not been confirmed. Oxidative stress and inferred DNA damage may play a critical role within the pathogenesis of respiratory diseases (Cheresh et al., 2013), and phthalates and their metabolites may exert a variety of genotoxic effects at DNA and chromosome level (Erkekoglu & Kocer-Gumusel, 2014), which may be inferred by increased generation of oxidative stress (Sicinska et al., 2021). Few *in vitro* studies addressed the effects of phthalates on airway epithelial cells to get insight into their potential mechanisms of inducing and promoting pathological events in the lung. These studies revealed that phthalate-induced mechanisms may encompass different modes of action that play key roles in airway remodeling and the development of lung diseases (Kim, 2019; Rafael-Vazquez et al., 2018; Shi et al., 2021).

As described by Frery et al. (2020), biomonitoring of occupational exposure to phthalates is highly topical due to the lack of knowledge on exposure levels and associated occupational health risks. While exposure may occur through inhalation, dermal and oral uptake, measurement of phthalate exposure studies rely on urinary phthalate metabolite analysis (Hines et al., 2011). A human exposure study thereby uncovered that the major uptake of phthalates occurred through inhalation and highlighted the importance of considering the deposited dose (Andersen et al., 2018).

Among others, dibutyl phthalate (DBP) has been classified as a substance of very high concern and has been subjected to stricter regulations. Even if no European-wide occupational threshold values have been established for phthalates, the Scientific Committee on Occupational Exposure Limits (SCOEL) propose an occupational exposure limit regarding DBP of 580 $\mu\text{g}/\text{m}^3$ over an 8 h time weighted average (TWA) (Hartwig et al., 2017). DBP is one of the majorly detected phthalates in gas and particle fractions in occupational settings and indoor environments, and exposure to DBP may exceed the European tolerable daily intake in the rubber industry and in phthalate manufacturing (Hines

et al., 2011). Notably, a meta-analysis on epidemiological data revealed *inter alia* an increased risk of developing lung cancer in occupationally exposed groups in the rubber manufacturing industry (Boniol et al., 2017). Furthermore, DBP may be of major interest for respiratory toxicity studies due to its high bioaccessibility upon inhalation (Wei et al., 2020). Despite the fact that DBP has been considered as a weakly mutagenic substance, standard studies on its *in vitro* genotoxic/mutagenic and *in vivo* carcinogenic effects are either contradictory, deficient in explanatory power and study design, or give ambiguous results on the role of metabolic activation, and are hence not sufficient to draw appropriate conclusions (Hartwig et al., 2017). In contrast to previous findings in animal models, *ex vivo* results in human mucosa cells of the upper aerodigestive tract (oropharynx and inferior nasal turbinate) revealed that DBP induces DNA damage as assessed by the alkaline version of comet assay (Kleinsasser et al., 2000). Of note, DNA strand break lesions were induced by DBP in human mucosal cells and in lymphocytes without metabolic activation (Hartwig et al., 2017; Kleinsasser et al., 2001). Nevertheless, increasing evidence suggests that DBP may induce genotoxic lesions in different human cell types, infer oxidative stress (Shi et al., 2021), and lead to serious oxidative DNA damage in living organisms (Du et al., 2015). A recent study showed clear genotoxic effects upon increasing DBP treatment in human peripheral blood mononuclear cells, including oxidative stress-related DNA base lesions in alarming concentrations detected in human blood (Sicinska et al., 2021). Taken together, these studies point towards the potential of DBP to be genotoxic in several human cell types. In general, knowledge on the biological effects of phthalates on lung cells is scarce and *in vitro* studies on lung cell models are limited to submerged conditions (Shi et al., 2021). This study aimed to consider the direct interaction of airway epithelium with DBP aerosols by exposing alveolar-like epithelial cells at the air-liquid interface (ALI) to different DBP concentrations for different time points. It uses the “CLOUD” exposure technique (Lenz et al., 2009) with homogeneous sedimentation of DBP particles onto the surface area of a cell layer for accurate dose control. To that scope, this study focused on the potential of DBP to infer genotoxic effects and oxidative stress on human alveolar A549 cells in exposure concentrations relevant at workplaces. To choose reasonable exposure conditions with occupational relevance, we compare the particle mass deposited during an experiment with the mass deposited on the tissue surface in the human lung. A particle deposition model (Ferron et al., 2013) yields deposition probability, inner surface area and tissue-deposited mass in the exposed lung regions (Karg et al., 2020). This approach provides an important link between the biological effects that are observed at ALI and deposition in the human lung.

2 | MATERIALS AND METHODS

2.1 | Exposure of human A549 cells at the air-liquid interface

Human A549 adenocarcinoma cells were purchased from the American Type Culture Collection (ATCC CCL-185). Cells were cultured in

RPMI-1640 medium (Gibco, Paisley, UK) supplemented with 10% inactivated fetal bovine serum (FBS, Sigma-Aldrich, St. Louis, MO), 1% L-alanine-L-glutamine (GlutaMAX, Gibco, Paisley, UK), 100 U/ml penicillin (Sigma-Aldrich, St. Louis, MO), and 100 µg/ml streptomycin (Sigma-Aldrich, St. Louis, MO). Either 150,000 (for micronucleus) or 250,000 (for all other experiments) cells were seeded on 6-well transwell inserts with a porous polyester membrane (24 mm diameter, 0.4 µm pore size, Corning, Kennebunk, ME). Twenty-four hours after seeding cells were further cultured at ALI for 24 h with fresh medium supplemented with 5% inactivated FBS for acclimatization, and afterwards exposed to different concentrations of DBP (Sigma-Aldrich, St. Louis, MO) in a VITROCELL® CLOUD 6 system (Vitrocell GmbH, Germany) equipped with an Aeroneb Pro vibrating mesh nebulizer (Aerogen, Ireland) generating liquid droplets of about 5 µm diameter. All operations were conducted according to the manufacturer recommendation. A detailed schematic prescription and explanation of the VITROCELL® CLOUD exposure system is given elsewhere (Ding et al., 2020). Briefly, cells grown on transwell supports were placed into wells containing complete medium without FBS at the bottom of the CLOUD chamber pre-heated to 37°C. DBP was brought into aqueous solution with 0.05% ethanol (AppliChem, Darmstadt, Germany) in medium without FBS (solvent) and cells treated with only solvent served as control. Four DBP solutions were used for nebulization: 0.07, 0.6, 5.6, and 50 µM, which correspond to 0.19, 1.67, 15.59, and 13.917 µg/ml, respectively. Notably, DBP has solubility in water between 10 and 13 µg/ml at 25 °C (ECB, 2003; Wang et al., 2018). A volume of 250 µl of the solvent or respective DBP solutions was applied to the nebulization unit. The liquid solution was nebulized for 1 min to ensure complete nebulization and the mist was allowed to sediment homogeneously onto the cells for 8 min each. A control group kept in the incubator during CLOUD exposure was used in each experiment as a reference to distinguish possible toxic effects derived from the exposure procedure. Cells were incubated for 4, 24, and 48 h at ALI after the exposure with complete medium supplemented with 3% inactivated FBS. Positive controls were used according to the performed assay as described below.

2.2 | Calculation of DBP particle deposition in the alveoli of the human lung

To estimate lung deposition of DBP at occupational settings, calculation of DBP particle deposition in the human lung of a male adult breathing via mouth without physical strain was conducted using the particle lung deposition model for polydisperse nonhygroscopic aerosols (Ferron et al., 2013) and the dose deposition calculation method by (Karg et al., 2020). Due to the lack of knowledge on size segregated particle association of DBP, deposition was calculated assuming a log-normal distribution for DBP particle sizes in the ultrafine to fine particle range for the recommended SCOEL threshold limit value (TLV) of 580 µg/m³ considering an occupational exposure over an 8 h TWA. The particle density was set to 1.05 g/cm³ for the pure DBP substance (Nitschke et al., 2017). The motivation of using a count median

diameter (CMD) in the nanosized particle range is supported by the fact that industrial processes, for example, vulcanization processes in the rubber manufacturing, or injection molding in the plastic processing industry, give rise to assume the emission of polydisperse particles in the ultrafine (~30 nm, ≤100 nm) and submicron (<1 µm) size range (Kim et al., 2013; Theriault et al., 2017) that may contain a panel of different phthalates in the respirable fractions (Szewczyńska et al., 2020). For polydisperse particles, a mean geometric standard deviation (GSD) of 1.9 was assumed, which is commonly found for process-generated particle populations (Kim et al., 2013). Detailed information on the calculations is given in the Supporting Information, Table SI, Table SII, and Figure S1.

2.3 | Measurement of DBP deposition

Based on a fluorescein measurement approach, a mean deposition in the VITROCELL® CLOUD 6 system on the total cell growth area of 16.8% was extrapolated (Lenz et al., 2014). Nebulization of 250 µl of a 5.6 µM DBP solution into the CLOUD would therefore result in a deposition of 2.4 ng/cm². To verify this data for DBP deposition in the experiments shown here, cells were exposed to a 5.6-µM deuterium labeled DBP (DBP-d4) (Sigma-Aldrich, St. Louis, MO) solution according to the previously described procedure due to the high background level of DBP. Immediately after cell exposure, the insert membranes were cut and transferred into ice cold methanol (LC-MS-grade, Sigma-Aldrich, St. Louis, MO) with 20% ultrapure water (Milli-Q®, Merck, Germany). Afterwards, the DBP-d4 samples were extracted in an ultrasonic bath for 3 min, centrifuged at 9390×g (Heraeus™ Biofuge Pico®, Thermo Scientific, Germany) for 5 min. The supernatant was directly transferred to fresh tubes and measured via liquid chromatography tandem mass spectrometry (LC-MS/MS). The LC-MS/MS system contains an Agilent 1290 UHPLC (Agilent Technologies) including a degasser, a binary pump, an autosampler, and a column compartment, coupled to an API 4000 Qtrap MS/MS system equipped with Turbo VTM Source (Sciex, USA). Detailed information on the LC-MS/MS system and the applied and analyzed parameters is given in the Supporting Information.

2.4 | Evaluation of cytotoxicity

To exclude cytotoxic effects in the evaluation of acute genotoxicity of DBP by means of the comet assay, cytotoxicity was evaluated 4 and 24 h after exposure in terms of lactate dehydrogenase (LDH) release into the basolateral medium and cellular metabolic activity with a resazurin based solution. LDH (Roche, Mannheim, Germany) and Resazurin (Invitrogen, Eugene, OA) assay were performed according to the manufacturer instructions. Cells treated with 2% Triton X-100 (Sigma-Aldrich, St. Louis, MO) 20 min before harvest served as positive controls and were used to determine the maximum LDH release. Normalization to the positive control gave the percentage of cytotoxicity. Resazurin assay was performed by incubating controls and

exposed cells with 10% resazurin solution in post incubation medium at 37°C and 5% CO₂ in a humidified incubator. Absorbances were detected with measurement/reference wavelengths of 493/620 nm for LDH and 571/620 nm for Resazurin assay in a Multiscan FC microplate reader (Thermo Scientific, China).

2.5 | Determination of malondialdehyde (MDA) content in supernatant

MDA content in the basolateral medium 4, 24, and 48 h after DBP exposure was measured to investigate oxidative-stress related lipid peroxidation. The samples were analyzed via the LC-MS/MS system described before with the detailed descriptions of the applied parameters given in the Supporting Information. Malondialdehyde tetra butylammonium salt (MDA-TBA), 2,4-dinitrophenylhydrazine (DNPH) and formic acid (FA) were purchased from Sigma-Aldrich (St. Louis, MO), while isotopic labeled 1,1,3,3-Tetraethoxypropane (1,3-d₂-TEP) was purchased from Cambridge Isotope Laboratories (Tewksbury, MA), and n-Hexane (HPLC-grade) was obtained from VWR (Leuven, Belgium). Malondialdehyde derivatization was performed according to a previous study (Wu et al., 2017). Detailed information on the sample preparation procedure, and the applied and analyzed parameters is given in the Supporting Information. The acquired MDA concentration in the samples was subtracted by the MDA background in the blank medium. A 700 µM tert-butyl hydroxy peroxide (t-BOOH, Merck, Darmstadt, Germany) solution served as positive control and was added 2 h prior to cell harvesting (Mateos et al., 2004).

2.6 | Single-cell gel electrophoresis (comet assay)

The mini-gel version of the alkaline comet assay was performed according to a previously published method (Di Bucchianico et al., 2017) to detect DNA damage derived from strand break lesions. Briefly, 4 and 24 h after exposure, control, and exposed A549 cells were harvested by trypsinization (0.05% Trypsin-EDTA, Sigma-Aldrich, St. Louis, MO) and diluted to a final concentration of 250,000 cells/ml. Cells treated with 30-µM hydrogen peroxide (H₂O₂, Merck, Darmstadt, Germany) for 5 min served as the positive control. Mini-gels on microscopy slides created with 1% low-melting point agarose (Sigma-Aldrich, St. Louis, MO) underwent 1 h of lysis, following 45 min of alkaline unwinding, subsequent electrophoretic separation of 25 min (270–300 mA, 1.2 V/cm²), and finally were subjected to a neutralizing step. The slides were air-dried at least overnight and DNA was stained with SYBR GOLD (Invitrogen, Eugene, OA) 1:10,000. A detailed description of the workflow and used buffers is given in the Supporting Information. Pictures were taken with a fluorescence microscope (10× magnification, BioTek Lionheart FX, Germany) and CometScore 2.0 software (TriTek Corp) was used to manually score at least 100 nucleoids per sample. Two replicate gels per sample were made (50 nucleoids per gel scored) and three independent exposures were performed. Results were

expressed as mean %DNA in tail corresponding to the mean of the mean replicate mean ± SEM (*n* = 3).

2.7 | Cytokinesis-block micronucleus cytochrome assay (CBMN-Cyt assay)

CBMN-Cyt assay was performed to assess the induced cytotoxicity, cytostasis, and chromosomal damage following 48 h exposure to different concentrations of DBP according to OECD guideline 487 (OECD, 2016). A549 cells were treated with 0.15 µg/ml mitomycin C (Cayman Chemical, Ann Arbor, MI) added to the basolateral medium as positive control. CBMN-Cyt assay was performed as described with minor modifications (Di Bucchianico et al., 2015). Briefly, A549 cells were seeded and treated with DPB as previously described. Cytochalasin B (Cayman Chemical, Ann Arbor, MI) was added to a final concentration of 5 µg/ml to the basolateral medium 24 h after exposure to prevent cytokinesis. CBMN-Cyt assay was performed after additional 24 h in order to ensure a 1.5–2 normal A549 cell cycle length considering a population doubling time of A549 between 20 and 24 h. A detailed description of the experimental procedure is given in the Supporting Information. As described (Di Bucchianico et al., 2017), 500 cells per sample were scored for cytostasis, apoptotic, necrotic, and mitotic cells. Chromosomal damage upon DBP treatment was analyzed in 1000 mono- and 1000 binucleated cells per independent replicate, leading to a total of 3000 mono- and 3000 binucleated cells scored per concentration. The number of MN in mono- and binucleated cells was considered to distinguish between aneuploidy and clastogenicity (Kirsch-Volders & Fenech, 2001; Rosefort et al., 2004). Nucleoplasmic bridges (NPB) arise from dicentric chromosomes because of misrepaired DNA strand breaks and/or telomere end-fusions, and nuclear buds (NBUD) are biomarkers of elimination of amplified DNA and/or DNA repair complexes.

2.8 | Statistical analysis

Statistical analysis was performed with SigmaPlot 13.0. The significance of the differences in the results was evaluated using one-way analysis of variance, followed by Tukey's multiple comparison post-hoc test. All comparisons were considered significantly different when *p* was <.05.

3 | RESULTS

3.1 | DBP-d4 deposition in the CLOUD and DBP particle deposition in the alveoli of the human lung

A comparison of the DBP particle lung deposition in the alveolar region predicted by the computer model and the measured deposition in the VITROCELL[®] CLOUD system is given in Table I. The particle

TABLE I Deposited mass of DBP [ng/cm^2] in the alveolar region of a human male person (computer modeling of DBP particles for different occupational scenarios) and in the cellular growth area of the CLOUD system (experimental DBP application)

Computer modeling of DBP particles				Experimental DBP application	
Occupational scenario	Particle CMD [nm]	Particle MMD [nm]	Alveolar deposition [ng/cm^2]	DBP concentration [μM]	CLOUD deposition [ng/cm^2]
Condensing from gas phase	30	103	0.76	0.07	0.03
High temperature emission	100	336	0.38	0.6	0.2
Mechanical machining	1000	3396	0.56	5.6	2.2
				50	20

Note: Calculations were conducted for different particle sizes mimicking different exposure scenarios (count median diameter, CMD, and corresponding mass median diameter, MMD) at the SCOEL TLV ($580 \mu\text{g}/\text{m}^3$) for an 8-h exposure. Deposition of the respective sprayed DBP concentrations was calculated by considering a deposition efficiency of 15.2% (according to LC-MS/MS measurements).

sizes reflect different airborne occupational exposure scenarios arising emitted during various industrial processes. Exposures to $580 \mu\text{g}/\text{m}^3$ of different DBP particle sizes over 8 h during a workday result in a corresponding alveolar deposition between 0.38 and $0.76 \text{ ng}/\text{cm}^2$. In the CLOUD, spraying of $250 \mu\text{l}$ of $5.6 \mu\text{M}$ DBP-d4 resulted in a deposition of $2.2 \text{ ng}/\text{cm}^2$, resulting in a deposition efficiency of 15.2%. Considering the measured deposition for a $5.6 \mu\text{M}$ DBP concentration, DBP nebulizing solutions of 0.07, 0.6, and $50 \mu\text{M}$ would result in 0.03, 0.2, and $20 \text{ ng}/\text{cm}^2$ deposition, respectively. Model calculation for the human lung showed the major mass being deposited in the alveolar region when inhaled by a person breathing calmly and orally (details see Supporting Information). When comparing the deposition per surface area of the computer model with the exposure system, the experimental DBP concentrations cover the scale of the numerical computer model calculations for exposures at the recommended SCOEL TLV of DBP ultrafine and fine particle sizes—therefore confirming the use of A549 alveolar-like epithelial cells for toxicological assessment at the experimental DBP concentrations.

3.2 | Cytotoxicity

Several methods were used to assess cytotoxic effects on A549 cells following DBP exposure. In general, Resazurin, LDH, and CBMN-Cyt assay did not show any significant decrease in cell viability or increase in cytotoxicity upon DBP treatment compared to the solvent control (Figure 1 and Figure S1). A slight decrease in cell viability could be detected after 4 h for all treated groups including the solvent control, while this effect was not observed after 24 h (Figure 1a). The viability 4 h after DBP treatment did not decrease below 11% of the solvent control. At both time points, the applied DBP concentrations did not induce cytotoxicity in A549 cells above 5% in comparison to the solvent control (Figure S1). As explained in the Supporting Information, solvent treatment did not affect cell viability or LDH release. Though not significant, CBMN-Cyt assay results indicated a slight decrease of the proliferative and mitotic capacity of A549 cells upon DBP treatment (Figure 1b,c). Additionally, a slight increase in apoptotic and necrotic cell number could be observed, with a tendency towards

apoptotic events (Figure 1d). No difference between cytotoxicity and cytotaxis occurred between the solvent and the incubator control (Figure S2a–d). The positive control represented by mitomycin C (MMC) treatment led to a significant decrease in the replication (Figure S2a) and mitotic index (Figure S2b) of A549 cells, while the frequency of necrotic cells increased (Figure S2c) and no significant increase in apoptotic events was observed (Figure S1d). In sum, the data confirmed sub-cytotoxic exposure conditions at all time points for the applied DBP concentrations in A549 cells.

3.3 | Single-cell gel electrophoresis (Comet) assay

Comet assay revealed that DBP treatment induces genotoxicity in the applied concentration range (Figure 2a). All DBP concentrations led to a significant increase of strand break lesions compared to the solvent control (5.4% DNA in tail) 24 h PE, ranging from 10.2% to 13.8% DNA in tail with increasing DBP concentration. The earlier time point (4 h PE) showed significant damage within intermediate concentrations compared to the solvent control (4.9% DNA in tail) and a range from 7.6% to 9.5% DNA in tail—a smaller potency of inducing DNA strand breaks in comparison to the later time point. Notably, the potency of the distinct DBP concentrations—comprising several magnitudes of orders—to induce genotoxicity, did not show a pronounced difference at the respective time points, although a slight increase with increasing DBP concentration was observed 24 h PE. The controls revealed that solvent treatment did not affect the detected basal level of % DNA in tail in A549 cells, while the positive control induced significant DNA damage (Figure 2b).

3.4 | MDA measurement

MDA concentrations 4 and 24 h after exposure were below the limit of quantification except for the respective t-BOOH positive controls (data not shown). Forty-eight hours after exposure, an increase of MDA with increasing DBP concentration was observed, resulting in significantly higher MDA levels with 0.2 and $2.2 \text{ ng}/\text{cm}^2$ DBP

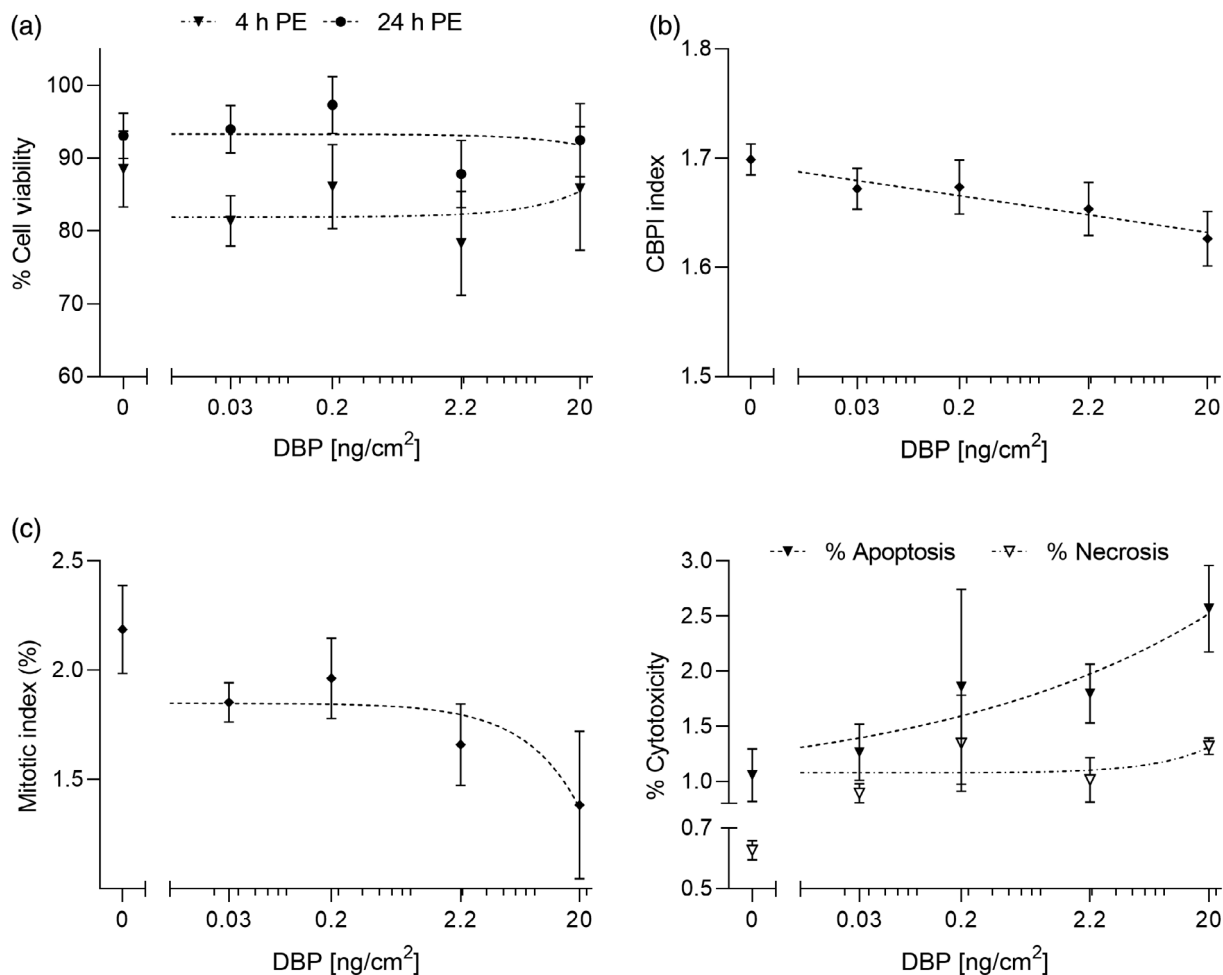


FIGURE 1 % Cell viability of A549 cells exposed to DBP [ng/cm^2] measured by metabolic activity via Resazurin assay upon 4 and 24 h post exposure (PE) ($n = 4$) (a). Proliferation determined by the cytokinesis block proliferation index (CBPI); the positive control 0.15 $\mu\text{g}/\text{ml}$ mitomycin C (MMC) showed a significant CBPI reduction to 1.50 ± 0.09 (Figure S2a) (b), cytostasis measured by the mitotic index (c), and cytotoxicity measured in % apoptosis and % necrosis (d) of A549 cells evaluated via CBMN-Cyt assay 48 h PE to DBP [ng/cm^2] ($n = 3$). Solvent control displayed as 0 ng/cm^2 . Data shown as mean \pm SEM

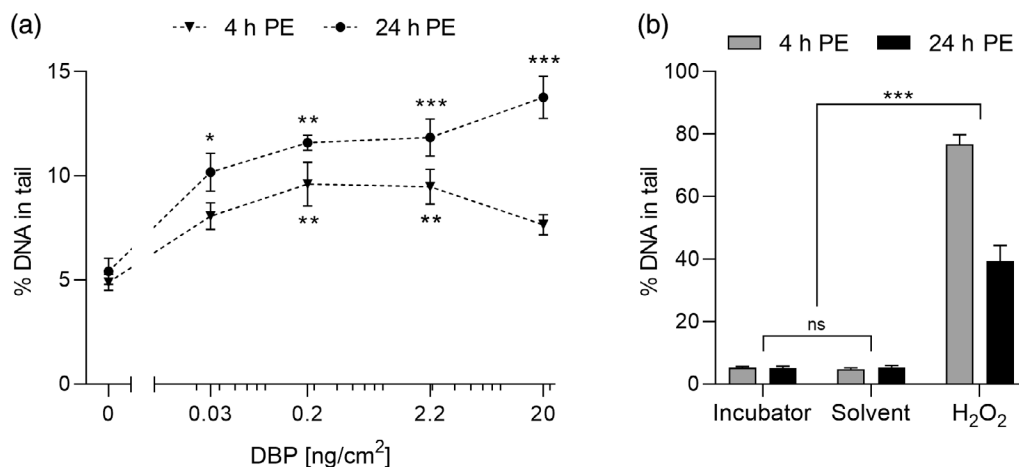


FIGURE 2 Comet assay results showing DNA damage 4 and 24 h PE in A549 cells as %DNA in tail upon DBP treatment [ng/cm^2] with significances determined using one-way ANOVA compared to solvent control (0 ng/cm^2 DBP) (a). Comparison of control groups; from left to right: Incubator, solvent, and 30 μM H_2O_2 positive control (b). Data shown as mean \pm SEM ($n = 3$). Statistical analysis via Tukey one-way ANOVA, * $p \leq .05$, ** $p \leq .01$, *** $p \leq .001$

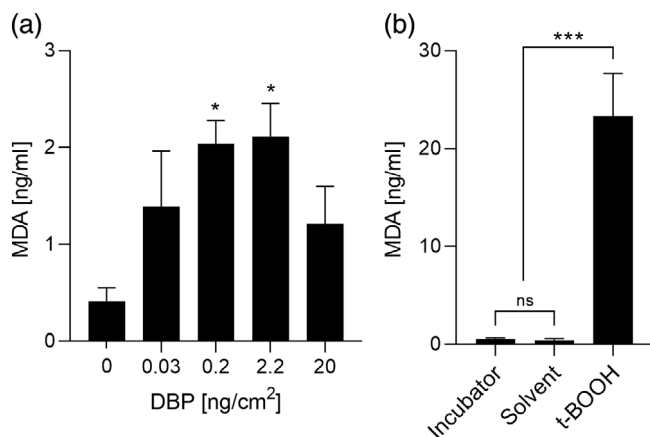


FIGURE 3 Malondialdehyde (MDA) [ng/ml] after 48 h in A549 cells exposed to DBP [ng/cm²] measured in supernatant via LC-MS/MS with significances determined using one-way ANOVA compared to solvent control (0 ng/cm² DBP) (a). Comparison of controls; from left to right: Incubator, solvent, and 700 μ M t-BOOH positive control (b) ($n = 4$). Data shown as mean \pm SEM. Statistical analysis via Tukey one-way ANOVA, * $p \leq .05$, *** $p \leq .001$

treatment (Figure 3a). Solvent and incubator controls showed no difference, while the positive control led to a significant MDA increase (Figure 3b).

3.5 | CBMN-Cyt assay

To identify genotoxic effects that may manifest in the genome and thereby provide a direct link to potential mutagenic and carcinogenic events, chromosomal instability was evaluated via CBMN-Cyt assay. Generally, the amount of chromosomal instability events in terms of MN, NPB, and NBUD increased with increasing DBP concentration (Figure 4a,b). DBP treatment led to a significant increase in the number of detected MN in mononucleated (19 ± 2.2) cells upon treatment with 20 ng/cm², while the number of MN in binucleated cells considerably increased upon treatment with 2.2 ng/cm² (21.2 ± 1.5) and 20 ng/cm² (22.2 ± 2.5) compared to the solvent control (7.0 ± 0.7 MN in mono- and 10.0 ± 0.2 MN in binucleated cells), revealing a potential role of DBP in the generation of aneuploidogenic as well as clastogenic events in airway epithelial cells (Figure 4a). No significant

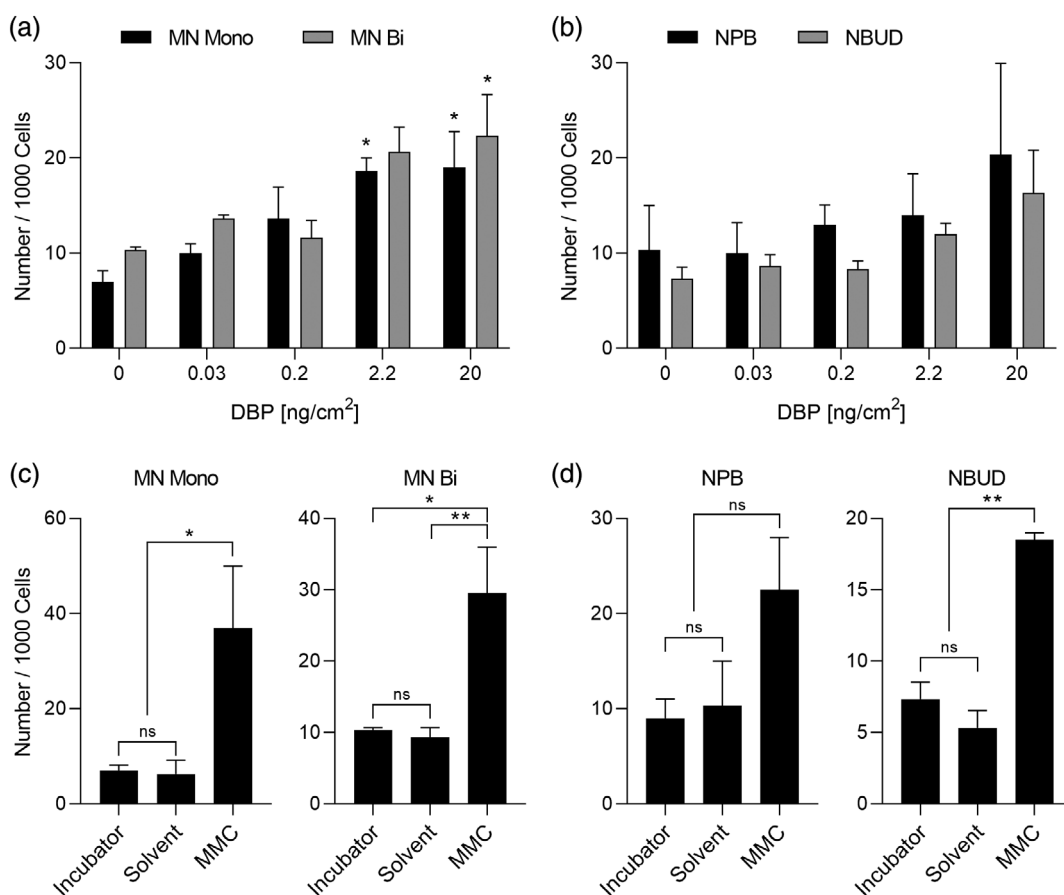


FIGURE 4 CBMN-Cyt assay results showing chromosomal instability after 48 h in A549 cells exposed to DBP [ng/cm²] as the number of events per 1000 cells in terms of micronuclei in mono- and binucleated cells (MN mono and MN bi) (a), nucleoplasmic bridges (NPB) and nuclear buds (NBUD) (b) with significances determined using one-way ANOVA compared to solvent control (0 ng/cm² DBP; $n = 3$). Comparison of control groups; from left to right: Incubator, solvent, and 0.15 μ g/ml mitomycin C (MMC) positive control for MN mono and MN bi (c), and NPB and NBUD (d). Data shown as mean \pm SEM. Statistical analysis via Tukey one-way ANOVA, * $p \leq .05$, ** $p \leq .01$

difference between solvent and incubator controls were detected, while the positive control mitomycin C induced a significant increase in MN in mono- and binucleated cells (Figure 4c), and NBUD frequency (Figure 4d), confirming the sensitivity of the test system.

4 | DISCUSSION

To which extent *in vitro* studies may reflect realistic conditions is always of concern, requiring approaches that lead toward more representative *in vitro* study designs to overcome these challenges. The deposition in the CLOUD system was in good agreement to literature (Lenz et al., 2014), revealed that the deposited doses range within the proposed 8 h SCOEL TLV, and allowed us to give mass-specific information on cellular responses of A549 cells to DBP exposure at occupationally relevant concentrations. Although this study confirms the workplace health risk of airborne phthalate exposure and implies the benefit of ALI *in vitro* systems, it has its limitations. In fact, it should be noted that this study considered a state of pure particle phase of DBP for the computer model calculations of alveolar deposition. With a vapor pressure of 2.01×10^{-5} kPa at 25°C (approx. corresponding to a DBP concentration of 300 $\mu\text{g}/\text{m}^3$ at atmospheric pressure; Wypych, 2017), the recommended SCOEL TLV regarding DBP of 580 $\mu\text{g}/\text{m}^3$ indicates that concentrations near and above the SCOEL would be representative of gas-particle mixtures that mainly result in particle/droplet deposition in the lung (Nitschke et al., 2017). The bioaccessibility of DBP upon inhalation may be very high in general, but only a low percentage may deposit in the alveolar region due to its physico-chemical properties. At workplaces, combinations of several different compounds and phthalates—depending on the industrial sectors – may occur, and gas phase exposure as well as distributions of DBP in different particle size ranges may play an important role for considering bioaccessibility (Wei et al., 2020). Nevertheless, DBP is predominantly used as an additive in the rubber industry (Frery et al., 2020), where threateningly high concentrations of ultrafine particles may be generated (Kim et al., 2013). DBP adsorbed to these particles may be transported into deep lung regions even at lower concentrations where the vapor saturation pressure is not reached. This study, hence, uncovered some limitations of current aerosol measurements at workplaces, as they mostly do not consider particle size distribution, associated phthalate concentration, and gas-particle partitioning of semi volatile organic compounds (SVOCs), which are important parameters for the prediction of SVOC lung deposition (Ching & Kajino, 2018).

The applied DBP concentrations (CLOUD deposition: 0.02–20 ng/cm^2) inferred genotoxic effects and oxidative stress even below the currently recommended SCOEL TLV of 580 $\mu\text{g}/\text{m}^3$ (calculated alveolar deposition: 0.38–0.76 ng/cm^2) in the A549 ALI model system, suggesting that a reevaluation of the current recommendations should be considered. Comet assay revealed significant DNA damaging effects upon treatment with DBP at concentration ranges relevant for workplaces. The induced strand break lesions start to arise immediately with application of the lowest concentration (0.03 ng/cm^2 DBP),

while increasing the DBP concentration in orders of magnitude does not lead to a considerable promotion of DNA damage. Phthalates have been shown to exhibit lung cell remodeling function in A549 cells, leading to changes in the epithelial phenotype with decreased surfactant expression and mesenchymal features (Rafael-Vazquez et al., 2018), suggesting that phthalates might lead to an accumulation of genetic alterations that could be transferred to morphological abnormalities (Ninomiya et al., 2006). It has recently been observed that DBP induces single and double DNA strand breaks that exceed the cellular DNA repair capacity as well as stronger DNA damaging effects compared to its metabolite monobutyl phthalate (Sicinska et al., 2021). After 4 h of DBP exposure, only treatment to the two intermediate concentrations (0.2 and 2.2 ng/cm^2) led to a statistically significant increase in %DNA in tail, while both the lowest and the highest tested concentration showed a slight but not significant increase compared to the solvent control under sub-cytotoxic conditions. Interestingly, the concentration-dependent trend after 24 h of exposure was not observed after the shorter exposure time. In fact, the increase of DNA strand break lesions after 24 h (compared to 4 h) suggests that the observed genotoxic effects might be a result of DBP metabolic activation, and that activated elements of the intrinsic cellular repair mechanisms of the DNA damage response system are not sufficient to overcome DBP/DBP-metabolite-induced DNA damage that might ultimately accumulate and lead to chromosomal aberrations (Chatterjee & Walker, 2017) in A549 cells. As a consequence, CBMN-Cyt assay was conducted to unravel genotoxic mechanisms that manifest in the genome. The number of MN in mono- and binucleated cells generally increased with increasing concentration and was significantly elevated upon DBP treatment with higher concentrations (2.2 and 20 ng/cm^2), which might point towards aneuploidogenic and clastogenic effects inferred in A549 cells upon DBP exposure. While aneuploidy-inducing chemicals lead to numerical chromosomal aberrations and follow a threshold activation pattern below which no effect is observed (Elhajouji et al., 1995; Elhajouji et al., 2011), clastogenic events encompass structural chromosomal aberrations in the form of DNA strand breaks and the threshold concept for clastogenicity is challenging. Indeed, positive results in both comet assay and micronucleus test, as occurring in the present study, could indicate clastogenic events, which were recently reported in the Guidance on aneugenicity assessment (Committee et al., 2021). Therefore, to further validate if DBP may act as a chemical aneugen and/or clastogen, the respective mechanisms need to be discriminated and a broader range of selected concentrations specifically below the applied DBP concentrations to identify the existence of a benchmark dose would be necessary. In accordance to previously published literature, comet assay seemed more sensitive to detect phthalate induced genetic damage (Al-Saleh et al., 2017). A critical knowledge gap is the extent of phthalate metabolism in human lungs (Kocbach Bolling et al., 2013), suggesting that inhalation toxicity should incorporate metabolite analysis to reveal the respective genotoxic potential. In this context, the frequently used A549 cell line could contribute to clarification of metabolic activation of DBP, since it represents a suitable *in vitro* model system for investigating the role of pulmonary

xenobiotic metabolism due to the expression and corresponding activity of CYP enzymes (Garcia-Canton et al., 2013; Oesch et al., 2019).

According to a recent study, DBP generates oxidative stress in A549 cells by increased reactive oxygen species (ROS) production and impairment of the antioxidant system, including elevated levels of MDA (Shi et al., 2021). Since DBP treatment led to an increase in MDA levels 48 h after treatment in A549 cells, persistent oxidative stress might be responsible for the observed genotoxic effects (Sicinska et al., 2021). A significant increase was observed upon 0.2 and 2.2 ng/cm² DBP treatment. At 20 ng/cm² DBP treatment, MDA levels decreased again (no significant reduction compared to 0.2 and 2.2 ng/cm²), which might be attributed to the activation of enzymatic pathways responsible for MDA metabolism or its reaction with biomolecules (Ayala et al., 2014), which could thereby explain the observed mutagenic effects in the CBMN-Cyt assay at the respective DBP concentrations. MDA is a product of ROS-induced lipid peroxidation and mutagenic in human cells (Niedernhofer et al., 2003), and MDA adduct formation with DNA and proteins are known initiators of various pathophysiological states in the lung (Sapkota & Wyatt, 2015). While numerous studies on airborne exposure to particulate matter and environmental contaminants have suggested the critical role of oxidative stress, ROS formation, lipid peroxidation, mitochondrial dysfunction, and impairment of the antioxidant system in pulmonary diseases (Kotha et al., 2014), DBP may cause toxic effects by inducing oxidative stress through distinct mechanisms, inter alia by ROS formation via aryl hydrocarbon receptor (AhR) signaling (Wojtowicz et al., 2017), or impairment of the antioxidant rescue system, consequently leading to oxidative injury and DNA damage (Shi et al., 2021; Sicinska et al., 2021). Additionally, the introduction of antioxidants might alleviate DBP induced airway remodeling mechanisms (Kuo et al., 2011). An *in vitro* study on mouse neurons revealed that specifically low DBP concentrations in the nanomolar range seem to promote oxidative stress, while concentrations in the micromolar range were prone to induce apoptosis (Wojtowicz et al., 2017). This might also in part explain the observed slight (not significant) increase in apoptotic events after 48 h and the concomitant decrease in MDA levels at 20 ng/cm² DBP. However, lipid peroxidation under subtoxic conditions usually initiates survival pathways by engagement of cellular antioxidative defense mechanisms (Ayala et al., 2014), which would presumably have resulted in increased MDA levels upon treatment with higher concentrations (20 ng/cm²). Additionally, it was shown that DBP treatment in A549 corrupts the antioxidative system by downregulation of antioxidant enzyme activity with a concomitant increase in MDA levels (Shi et al., 2021). Given the fact that the highest DBP concentration prepared (50 μM) is already slightly surpassing the solubility limit, the decrease in MDA levels could additionally be affected by substance precipitation and hence correspond to an artifactual effect.

Phthalates have been shown to interact with the AhR (Kruger et al., 2008), and several studies were indicating its engagement in the promotion of phthalate-induced cancer (Hsieh et al., 2012). However, it has not yet been described which modes of action selectively account for phthalate toxicity in humans (Wang et al., 2019). although, it has been shown that DBP is capable of inducing aneuploidy (Benli

et al., 2016) and oxidative DNA lesions (Sicinska et al., 2021), up to our knowledge, this is the first time that DBP has been observed to generate aneuploidy/clastogenicity and lipid peroxidation in human lung cells at ALI culture conditions. Given the fact that DBP occurs in combination with other phthalates and is used as an additive in synthetic polymers such as plastics, inhalable microplastic particle fractions might contain alarming high amounts of phthalates (Campanale et al., 2020), suggesting that a combined toxicological screening of inhalation toxicity might be of special relevance.

5 | CONCLUSION

To evaluate potential adverse health effects of phthalates upon inhalation exposure, the current study evaluated DBP toxicity in human A549 alveolar-like cells at the ALI. It showed that DBP induces oxidative stress and exerts genotoxic effects on the lung cells on different levels—ranging from DNA strand breaks to chromosomal abnormalities. The comparison of computer-modeled lung and *in vitro* measured ALI deposition allowed the use of cellular concentrations of DBP that are comparable to particle deposited mass in the alveolar region encountered in occupational settings. DBP was potent to generate considerable DNA damage and led to increased MDA levels, suggesting a possible role of oxidative stress in the observed genotoxic effects. By combining the assessment of DBP toxicity, and cellular and computer modeling of lung deposition, this study may provide further insight into the health risk of occupational inhalation exposure to phthalates. Since even low concentrations of DBP may be potentially genotoxic to the human epithelium, inhalation toxicity of phthalates in humans in the context of airborne exposure dimensions (gas and particle phase) should gain further attention. Future *in vitro* studies should strive for experimental approaches that more closely represent real exposure scenarios, such as long-term exposures translated into epithelial cell culture models with phenotypic similarities to the human airway (including alveolar structure) with an adequate time resolution and SVOC partitioning representative of occupational inhalation exposure.

ACKNOWLEDGMENTS

We acknowledge the funding from the German Social Accident Insurance (DGUV) as part of the project FP425 (2019). Open access funding enabled and organized by Projekt DEAL.

CONFLICT OF INTEREST

The authors declare that they have no conflict of interest.

AUTHOR CONTRIBUTIONS

Stephanie Binder was involved in the experimental design, performed the experiments, supported the modeling studies, and wrote the first version of the manuscript. Xin Cao and Evelyn Kuhn took part of the experimental work. Stefanie Bauer, Narges Rastak, and Martin Sklorz contributed to the interpretation of the results and revised the manuscript. George C. Dragan initiated the project. George Ferron and

Erwin Karg performed the deposition modeling studies. Sebastian Oeder, Christian Monsé, and Dietmar Breuer were involved in the project evaluation and manuscript preparation. Sebastiano Di Bucchianico initiated the study, supervised the experiments, was involved in data interpretation, and manuscript preparation. Ralf Zimmermann provided access to all facilities, was involved in data interpretation and manuscript preparation. All authors read and approved the final manuscript.

REFERENCES

- Al-Saleh, I., Al-Rajudi, T., Al-Qudaihi, G. & Manogaran, P. (2017) Evaluating the potential genotoxicity of phthalates esters (PAEs) in perfumes using in vitro assays. *Environmental Science and Pollution Research International*, 24(30), 23903–23914. <https://doi.org/10.1007/s11356-017-9978-1>
- Andersen, C., Kraus, A.M., Eriksson, A.C., Jakobsson, J., Löndahl, J., Nielsen, J. et al. (2018) Inhalation and dermal uptake of particle and gas-phase phthalates—a human exposure study. *Environmental Science & Technology*, 52(21), 12792–12800. <https://doi.org/10.1021/acs.est.8b03761>
- Ayala, A., Munoz, M.F. & Arguelles, S. (2014) Lipid peroxidation: production, metabolism, and signaling mechanisms of malondialdehyde and 4-hydroxy-2-nonenal. *Oxidative Medicine and Cellular Longevity*, 2014, 360438–360431. <https://doi.org/10.1155/2014/360438>
- Benli, A.C., Erkmen, B. & Erkoc, F. (2016) Genotoxicity of sub-lethal di-n-butyl phthalate (DBP) in Nile tilapia (*Oreochromis niloticus*). *Arhiv za Higijenu Rada i Toksikologiju*, 67(1), 25–30. <https://doi.org/10.1515/aiht-2016-67-2723>
- Boniol, M., Koechlin, A. & Boyle, P. (2017) Meta-analysis of occupational exposures in the rubber manufacturing industry and risk of cancer. *International Journal of Epidemiology*, 46(6), 1940–1947. <https://doi.org/10.1093/ije/dyx146>
- Campanale, C., Massarelli, C., Savino, I., Locaputo, V. & Uricchio, V.F. (2020) A detailed review study on potential effects of microplastics and additives of concern on human health. *International Journal of Environmental Research and Public Health*, 17(4), 1212. <https://doi.org/10.3390/ijerph17041212>
- Chatterjee, N. & Walker, G.C. (2017) Mechanisms of DNA damage, repair, and mutagenesis. *Environmental and Molecular Mutagenesis*, 58(5), 235–263. <https://doi.org/10.1002/em.22087>
- Cheresh, P., Kim, S.J., Tulasiram, S. & Kamp, D.W. (2013) Oxidative stress and pulmonary fibrosis. *Biochimica et Biophysica Acta*, 1832(7), 1028–1040. <https://doi.org/10.1016/j.bbadis.2012.11.021>
- Chi, C., Xia, M., Zhou, C., Wang, X., Weng, M. & Shen, X. (2017) Determination of 15 phthalate esters in air by gas-phase and particle-phase simultaneous sampling. *Journal of Environmental Sciences (China)*, 55, 137–145. <https://doi.org/10.1016/j.jes.2016.01.036>
- Ching, J. & Kajino, M. (2018) Aerosol mixing state matters for particles deposition in human respiratory system. *Scientific Reports*, 8(1), 8864. <https://doi.org/10.1038/s41598-018-27156-z>
- Committee, E.S., More, S.J., Bampidis, V., Bragard, C., Halldorsson, T.I., Hernandez-Jerez, A.F. et al. (2021) Guidance on aneugenicity assessment. *EFSA Journal*, 19(8), e06770. <https://doi.org/10.2903/j.efsa.2021.6770>
- Di Bucchianico, S., Cappellini, F., Le Bihanic, F., Zhang, Y., Dreij, K. & Karlsson, H.L. (2017) Genotoxicity of TiO₂ nanoparticles assessed by mini-gel comet assay and micronucleus scoring with flow cytometry. *Mutagenesis*, 32(1), 127–137. <https://doi.org/10.1093/mutage/gew030>
- Di Bucchianico, S., Migliore, L., Marsili, P., Vergari, C., Giammanco, F. & Giorgetti, E. (2015) Cyto- and genotoxicity assessment of Gold nanoparticles obtained by laser ablation in A549 lung adenocarcinoma cells. *Journal of Nanoparticle Research*, 17(5), 213. <https://doi.org/10.1007/s11051-015-3023-4>
- Ding, Y., Weindl, P., Lenz, A.G., Mayer, P., Krebs, T. & Schmid, O. (2020) Quartz crystal microbalances (QCM) are suitable for real-time dosimetry in nanotoxicological studies using VITROCELL(R)Cloud cell exposure systems. *Particle and Fibre Toxicology*, 17(1), 44. <https://doi.org/10.1186/s12989-020-00376-w>
- Du, L., Li, G., Liu, M., Li, Y., Yin, S., Zhao, J. et al. (2015) Evaluation of DNA damage and antioxidant system induced by di-n-butyl phthalates exposure in earthworms (*Eisenia fetida*). *Ecotoxicology and Environmental Safety*, 115, 75–82. <https://doi.org/10.1016/j.ecoenv.2015.01.031>
- ECB. (2003) European Union risk assessment report on Dibutyl phthalate—addendum to the environmental section 2004. In: SJM, B. G.H., Allanou, R., Berthault, F., de Bruijn, J., Luotamo, M., Musset, C. et al. (Eds.) *European chemicals agency (ECHA)*, Vol. 29. Luxembourg: Office for Official Publications of the European Communities.
- Elhajouji, A., Lukamowicz, M., Cammerer, Z. & Kirsch-Volders, M. (2011) Potential thresholds for genotoxic effects by micronucleus scoring. *Mutagenesis*, 26(1), 199–204. <https://doi.org/10.1093/mutage/geq089>
- Elhajouji, A., Van Hummelen, P. & Kirsch-Volders, M. (1995) Indications for a threshold of chemically-induced aneuploidy in vitro in human lymphocytes. *Environmental and Molecular Mutagenesis*, 26(4), 292–304. <https://doi.org/10.1002/em.2850260405>
- Erkekoglu, P. & Kocer-Gumusel, B. (2014) Genotoxicity of phthalates. *Toxicology Mechanisms and Methods*, 24(9), 616–626. <https://doi.org/10.3109/15376516.2014.960987>
- Ferron, G.A., Upadhyay, S., Zimmermann, R. & Karg, E. (2013) Model of the deposition of aerosol particles in the respiratory tract of the rat. II. Hygroscopic particle deposition. *J Aerosol Med Pulm Drug Deliv*, 26(2), 101–119. <https://doi.org/10.1089/jamp.2011.0965>
- Frery, N., Santonen, T., Porras, S.P., Fucic, A., Leso, V., Bousoumah, R. et al. (2020) Biomonitoring of occupational exposure to phthalates: a systematic review. *International Journal of Hygiene and Environmental Health*, 229, 113548. <https://doi.org/10.1016/j.ijheh.2020.113548>
- Garcia-Canton, C., Minet, E., Anadon, A. & Meredith, C. (2013) Metabolic characterization of cell systems used in vitro toxicology testing: lung cell system BEAS-2B as a working example. *Toxicology In Vitro*, 27(6), 1719–1727. <https://doi.org/10.1016/j.tiv.2013.05.001>
- Hartwig, A., Papameletiou, D., & Klein, C.L. (2017) Recommendation from the Scientific Committee on Occupational Exposure Limits—SCOEL/REC/143 Di-n-butyl phthalate. Directorate-General for Employment, Social Affairs and Inclusion (European Commission), SCOEL, Luxembourg: Publications Office of the European Union. doi: <https://doi.org/10.2767/972673>
- Hines, C.J., Hopf, N.B., Deddens, J.A., Silva, M.J. & Calafat, A.M. (2011) Estimated daily intake of phthalates in occupationally exposed groups. *Journal of Exposure Science & Environmental Epidemiology*, 21(2), 133–141. <https://doi.org/10.1038/jes.2009.62>
- Hou, J., Yin, W., Li, P., Hu, C., Xu, T., Cheng, J. et al. (2020) Joint effect of polycyclic aromatic hydrocarbons and phthalates exposure on telomere length and lung function. *Journal of Hazardous Materials*, 386, 121663. <https://doi.org/10.1016/j.jhazmat.2019.121663>
- Hsieh, T.H., Tsai, C.F., Hsu, C.Y., Kuo, P.L., Lee, J.N., Chai, C.Y. et al. (2012) Phthalates induce proliferation and invasiveness of estrogen receptor-negative breast cancer through the AhR/HDAC6/c-Myc signaling pathway. *The FASEB Journal*, 26(2), 778–787. <https://doi.org/10.1096/fj.11-191742>
- Karg, E.W., Ferron, G.A., Bauer, S., Di Bucchianico, S. & Zimmermann, R. (2020) Is the particle deposition in a cell exposure facility comparable to the lungs? A computer model approach. *Aerosol Science and Technology*, 54(6), 668–684. <https://doi.org/10.1080/02786826.2020.1724868>
- Kashyap, D. & Agarwal, T. (2018) Concentration and factors affecting the distribution of phthalates in the air and dust: a global scenario. *Science of the Total Environment*, 635, 817–827. <https://doi.org/10.1016/j.scitotenv.2018.04.158>

- Kim, B., Lee, J.S., Choi, B.S., Park, S.Y., Yoon, J.H. & Kim, H. (2013) Ultrafine particle characteristics in a rubber manufacturing factory. *The Annals of Occupational Hygiene*, 57(6), 728–739. <https://doi.org/10.1093/annhyg/mes102>
- Kim, J.H. (2019) Di(2-ethylhexyl) phthalate promotes lung cancer cell line A549 progression via Wnt/beta-catenin signaling. *The Journal of Toxicological Sciences*, 44(4), 237–244. <https://doi.org/10.2131/jts.44.237>
- Kirsch-Volders, M. & Fenech, M. (2001) Inclusion of micronuclei in non-divided mononuclear lymphocytes and necrosis/apoptosis may provide a more comprehensive cytokinesis block micronucleus assay for biomonitoring purposes. *Mutagenesis*, 16(1), 51–58. <https://doi.org/10.1093/mutage/16.1.51>
- Kleinsasser, N.H., Kastenbauer, E.R., Weissacher, H., Muenzenrieder, R. K. & Harreus, U.A. (2000) Phthalates demonstrate genotoxicity on human mucosa of the upper aerodigestive tract. *Environmental and Molecular Mutagenesis*, 35(1), 9–12. [https://doi.org/10.1002/\(sici\)1098-2280\(2000\)35:1<9::aid-em2>3.0.co;2-1](https://doi.org/10.1002/(sici)1098-2280(2000)35:1<9::aid-em2>3.0.co;2-1)
- Kleinsasser, N.H., Wallner, B.C., Kastenbauer, E.R., Weissacher, H. & Harreus, U.A. (2001) Genotoxicity of di-butyl-phthalate and di-isobutyl-phthalate in human lymphocytes and mucosal cells. *Teratogenesis, Carcinogenesis, and Mutagenesis*, 21(3), 189–196. <https://doi.org/10.1002/tcm.1007>
- Kocbach Bolling, A., Holme, J.A., Bornehag, C.G., Nygaard, U.C., Bertelsen, R.J., Nånberg, E. et al. (2013) Pulmonary phthalate exposure and asthma—is PPAR a plausible mechanistic link? *EXCLI Journal*, 12, 733–759.
- Kotha, S.R., Gurney, T., Magalang, M., Hund, T., Satoskar, A. & Mohler, P. (2014) Mitochondrial lipid peroxidation in lung damage and disease. In: Natarajan, V. & Parinandi, N. (Eds.) *Respiratory medicine*, Vol. 15. New York: Humana Press.
- Kruger, T., Long, M. & Bonefeld-Jorgensen, E.C. (2008) Plastic components affect the activation of the aryl hydrocarbon and the androgen receptor. *Toxicology*, 246(2–3), 112–123. <https://doi.org/10.1016/j.tox.2007.12.028>
- Kuo, P.L., Hsu, Y.L., Huang, M.S., Tsai, M.J. & Ko, Y.C. (2011) Ginger suppresses phthalate ester-induced airway remodeling. *Journal of Agricultural and Food Chemistry*, 59(7), 3429–3438. <https://doi.org/10.1021/jf1049485>
- Lenz, A.G., Karg, E., Lentner, B., Dittrich, V., Brandenberger, C., Rothen-Rutishauser, B. et al. (2009) A dose-controlled system for air-liquid interface cell exposure and application to zinc oxide nanoparticles. *Particle and Fibre Toxicology*, 6, 32. <https://doi.org/10.1186/1743-8977-6-32>
- Lenz, A.G., Stoeger, T., Cei, D., Schmidmeir, M., Semren, N., Burgstaller, G. et al. (2014) Efficient bioactive delivery of aerosolized drugs to human pulmonary epithelial cells cultured in air-liquid interface conditions. *American Journal of Respiratory Cell and Molecular Biology*, 51(4), 526–535. <https://doi.org/10.1165/rcmb.2013-0479OC>
- Mateos, R., Goya, L. & Bravo, L. (2004) Determination of malondialdehyde by liquid chromatography as the 2,4-dinitrophenylhydrazone derivative: a marker for oxidative stress in cell cultures of human hepatoma HepG2. *Journal of Chromatography. B, Analytical Technologies in the Biomedical and Life Sciences*, 805(1), 33–39. <https://doi.org/10.1016/j.jchromb.2004.02.004>
- Niedernhofer, L.J., Daniels, J.S., Rouzer, C.A., Greene, R.E. & Marnett, L.J. (2003) Malondialdehyde, a product of lipid peroxidation, is mutagenic in human cells. *The Journal of Biological Chemistry*, 278(33), 31426–31433. <https://doi.org/10.1074/jbc.M212549200>
- Ninomiya, H., Nomura, K., Satoh, Y., Okumura, S., Nakagawa, K., Fujiwara, M. et al. (2006) Genetic instability in lung cancer: concurrent analysis of chromosomal, mini- and microsatellite instability and loss of heterozygosity. *British Journal of Cancer*, 94(10), 1485–1491. <https://doi.org/10.1038/sj.bjc.6603121>
- Nitschke L, Breuer D, Frenzen A, Heinrich B, Hebisch R, Brock T.H, et al. (2017) Phthalates—Method for the determination of phthalates in workplace air using gas chromatography mass spectrometry (GC-MS) [Phthalate – Methode zur Bestimmung von Phthalaten in der Luft am Arbeitsplatz mittels Gaschromatographie-Massenspektrometrie (GC-MS)] Air Monitoring Methods in German language Phthalate – Methode zur Bestimmung von Phthalaten in der Luft am Arbeitsplatz mittels Gaschromatographie-Massenspektrometrie (GC-MS). The MAK Collection for Occupational Health and Safety 2:1091–1111 doi: <https://doi.org/10.1002/3527600418.am8461d0019>
- OECD. (2016) *Guidelines for the testing of chemicals, in vitro mammalian cell micronucleus test no. 487. Section 4: health effects*. Paris: OECD Publishing. <https://doi.org/10.1787/20745788>
- Oesch, F., Fabian, E. & Landsiedel, R. (2019) Xenobiotica-metabolizing enzymes in the lung of experimental animals, man and in human lung models. *Archives of Toxicology*, 93(12), 3419–3489. <https://doi.org/10.1007/s00204-019-02602-7>
- Rafael-Vazquez, L., Garcia-Trejo, S., Aztatzi-Aguilar, O.G., Bazan-Perkins, B. & Quintanilla-Vega, B. (2018) Exposure to diethylhexyl phthalate (DEHP) and monoethylhexyl phthalate (MEHP) promotes the loss of alveolar epithelial phenotype of A549 cells. *Toxicology Letters*, 294, 135–144. <https://doi.org/10.1016/j.toxlet.2018.05.012>
- Rosefort, C., Fauth, E. & Zankl, H. (2004) Micronuclei induced by aneugens and clastogens in mononucleate and binucleate cells using the cytokinesis block assay. *Mutagenesis*, 19(4), 277–284. <https://doi.org/10.1093/mutage/geh028>
- Sapkota, M. & Wyatt, T.A. (2015) Alcohol, aldehydes, adducts and airways. *Biomolecules*, 5(4), 2987–3008. <https://doi.org/10.3390/biom5042987>
- Shi, Q., Tang, J., Wang, L., Liu, R. & Giesy, J.P. (2021) Combined cytotoxicity of polystyrene nanoplastics and phthalate esters on human lung epithelial A549 cells and its mechanism. *Ecotoxicology and Environmental Safety*, 213, 112041. <https://doi.org/10.1016/j.ecoenv.2021.112041>
- Sicinska, P., Mokra, K., Wozniak, K., Michalowicz, J. & Bukowska, B. (2021) Genotoxic risk assessment and mechanism of DNA damage induced by phthalates and their metabolites in human peripheral blood mononuclear cells. *Scientific Reports*, 11(1), 1658. <https://doi.org/10.1038/s41598-020-79932-5>
- Szewczyńska, M., Pośniak, M. & Dobrzyńska, E. (2020) Determination of phthalates in particulate matter and gaseous phase emitted into the air of the working environment. *International Journal of Environmental Science and Technology*, 17(1735–1472), 175–186. <https://doi.org/10.1007/s13762-019-02435-y>
- Therhault, M., Yoeuth, S., Matar, J., Martin, J., Bello, D. & Barry, C. (2017) Investigation of nanoparticles emitted when injection molding neat and additive-filled polypropylene and polycarbonate. *AIP Conference Proceedings*, 1914(1), 140008. <https://doi.org/10.1063/1.5016773>
- Wang, Q., Cai, C., Wang, M., Guo, Q., Wang, B., Luo, W. et al. (2018) Efficient Photocatalytic degradation of malachite green in seawater by the hybrid of zinc-oxide Nanorods grown on three-dimensional (3D) reduced Graphene oxide(RGO)/Ni foam. *Materials (Basel)*, 11(6), 1004. <https://doi.org/10.3390/ma11061004>
- Wang, Y., Zhu, H. & Kannan, K. (2019) A review of biomonitoring of phthalate exposures. *Toxics*, 7(2), 21. <https://doi.org/10.3390/toxics7020021>
- Wang, Y.C., Chen, H.S., Long, C.Y., Tsai, C.F., Hsieh, T.H., Hsu, C.Y. et al. (2012) Possible mechanism of phthalates-induced tumorigenesis. *The Kaohsiung Journal of Medical Sciences*, 28(7 Suppl), S22–S27. <https://doi.org/10.1016/j.kjms.2012.05.006>
- Warner, G.R. & Flaws, J.A. (2018) Bisphenol a and phthalates: how environmental chemicals are reshaping toxicology. *Toxicological Sciences*, 166(2), 246–249. <https://doi.org/10.1093/toxsci/kfy232>
- Wei, W., Ramalho, O. & Mandin, C. (2020) Modeling the bioaccessibility of inhaled semivolatile organic compounds in the human respiratory tract. *International Journal of Hygiene and Environmental Health*, 224, 113436. <https://doi.org/10.1016/j.ijheh.2019.113436>
- Wojtowicz, A.K., Szychowski, K.A., Wnuk, A. & Kajta, M. (2017) Dibutyl phthalate (DBP)-induced apoptosis and neurotoxicity are mediated via the aryl hydrocarbon receptor (AhR) but not by estrogen receptor alpha (ERalpha), estrogen receptor beta (ERbeta), or peroxisome proliferator-activated receptor gamma (PPARgamma) in mouse cortical

- neurons. *Neurotoxicity Research*, 31(1), 77–89. <https://doi.org/10.1007/s12640-016-9665-x>
- Wu, X., Lintemann, J., Klingbeil, S., Li, J., Wang, H., Kuhn, E. et al. (2017) Determination of air pollution-related biomarkers of exposure in urine of travellers between Germany and China using liquid chromatographic and liquid chromatographic-mass spectrometric methods: a pilot study. *Biomarkers*, 22(6), 525–536. <https://doi.org/10.1080/1354750X.2017.1306753>
- Wypych, A. (2017) *Databook of plastiziers*, 2nd edition. Canada: Elsevier, ChemTec Publishing, pp. 435–560. <https://doi.org/10.1016/B978-1-895198-96-6.50028-6>
- Zoeller, R.T., Brown, T.R., Doan, L.L., Gore, A.C., Skakkebaek, N.E., Soto, A. M. et al. (2012) Endocrine-disrupting chemicals and public health protection: a statement of principles from The Endocrine Society. *Endocrinology*, 153(9), 4097–4110. <https://doi.org/10.1210/en.2012-1422>

SUPPORTING INFORMATION

Additional supporting information may be found in the online version of the article at the publisher's website.

How to cite this article: Binder, S., Cao, X., Bauer, S., Rastak, N., Kuhn, E., Dragan, G.C. et al. (2021) In vitro genotoxicity of dibutyl phthalate on A549 lung cells at air–liquid interface in exposure concentrations relevant at workplaces. *Environmental and Molecular Mutagenesis*, 1–12. Available from: <https://doi.org/10.1002/em.22464>